

UCSF

UC San Francisco Previously Published Works

Title

Regulation of leading edge microtubule and actin dynamics downstream of Rac1.

Permalink

<https://escholarship.org/uc/item/1d1350cb>

Journal

The Journal of cell biology, 161(5)

ISSN

0021-9525

Authors

Wittmann, Torsten

Bokoch, Gary M

Waterman-Storer, Clare M

Publication Date

2003-06-01

DOI

10.1083/jcb.200303082

Peer reviewed

Regulation of leading edge microtubule and actin dynamics downstream of Rac1

Torsten Wittmann,¹ Gary M. Bokoch,² and Clare M. Waterman-Storer¹

¹Department of Cell Biology and Institute for Childhood and Neglected Diseases, and ²Department of Immunology, The Scripps Research Institute, La Jolla, CA 92037

Actin in migrating cells is regulated by Rho GTPases. However, Rho proteins might also affect microtubules (MTs). Here, we used time-lapse microscopy of PtK1 cells to examine MT regulation downstream of Rac1. In these cells, "pioneer" MTs growing into leading-edge protrusions exhibited a decreased catastrophe frequency and an increased time in growth as compared with MTs further from the leading edge. Constitutively active Rac1(Q61L) promoted pioneer behavior in most MTs, whereas dominant-negative Rac1(T17N) eliminated pioneer

MTs, indicating that Rac1 is a regulator of MT dynamics *in vivo*. Rac1(Q61L) also enhanced MT turnover through stimulation of MT retrograde flow and breakage. Inhibition of p21-activated kinases (Paks), downstream effectors of Rac1, inhibited Rac1(Q61L)-induced MT growth and retrograde flow. In addition, Rac1(Q61L) promoted lamellipodial actin polymerization and Pak-dependent retrograde flow. Together, these results indicate coordinated regulation of the two cytoskeletal systems in the leading edge of migrating cells.

Introduction

In migrating tissue cells, directed cell motility requires polarized organization and dynamics of both the actin and microtubule (MT)* cytoskeletons. Protrusion of the leading-edge lamellipodium relies on continuous actin polymerization into a dense, cross-linked meshwork of filaments, which, as it polymerizes, moves away from the cell edge in a process called retrograde flow (Small et al., 2002). Actin polymerization in lamellipodia is regulated by Rac1, a small Rho family small GTPase (Hall, 1998; Ridley, 2001).

In interphase cells, MTs are organized by the centrosome where many minus ends are anchored, whereas MT plus ends extend into the periphery. MT plus ends exhibit a non-equilibrium polymerization behavior referred to as dynamic instability (Desai and Mitchison, 1997), the stochastic switching between phases of growth and shortening. This is described by four parameters: the rates of growth and shortening and the transition frequencies from growth to shortening (catastrophe frequency) and from shortening to growth (rescue

frequency). *In vivo*, MT-associated proteins, MT plus-end binding proteins, and soluble factors regulate dynamic instability. In migrating cells, the MT cytoskeleton is polarized. In fibroblasts and endothelial cells, the centrosome and most MTs are oriented toward the leading edge (Wittmann and Waterman-Storer, 2001), and in epithelial cells, MT plus ends close to the leading edge often grow more persistently than MTs further back in the cell body (Waterman-Storer and Salmon, 1997; Wadsworth, 1999; Ballestrem et al., 2000).

Recent evidence suggests that MTs can also be targets of Rho GTPase regulation. Cdc42 mediates the cytoplasmic dynein-dependent orientation of the centrosome toward the leading edge (Etienne-Manneville and Hall, 2001; Palazzo et al., 2001a), whereas RhoA and its effector mDia regulate the formation of stable MTs (Palazzo et al., 2001b). In addition, a recent report showed that stimulation of HeLa cells with EGF results in phosphorylation of Op18/stathmin in a Rac1- and p21-activated serine/threonine kinase-dependent manner (Daub et al., 2001; Bokoch, 2003). Because Op18/stathmin is an inhibitor of MT polymerization that is inactivated by phosphorylation, we used time-lapse fluorescence microscopy to investigate whether signaling through Rac1 and p21-activated kinases (Paks) could regulate MT dynamic instability *in vivo*. We find that constitutively active Rac1(Q61L) promotes Pak-dependent MT growth and turnover. Similarly, Pak also mediates lamellipodial actin polymerization and retrograde flow downstream of Rac1(Q61L), demonstrating a coordinated

The online version of this article includes supplemental material.

Address correspondence to Clare M. Waterman-Storer, The Scripps Research Institute, Dept. of Cell Biology, CB 163, 10550 North Torrey Pines Rd., La Jolla, CA 92037. Tel.: (858) 784-9764. Fax: (858) 784-9779. E-mail: waterman@scripps.edu

*Abbreviations used in this paper: MT, microtubule; Pak, p21-activated kinase; PBD/ID(H83L), mutated p21-binding and autoinhibitory domains of Pak1.

Key words: cell motility; cytoskeleton; tubulin; Rho GTPases; p21-activated kinase

Table I. MT dynamic instability parameters in PtK1 cells

		Control "Central" MTs	Control "Pioneer" MTs	PBD/ID(H83L)	Rac1(Q61L)	Rac1(Q61L)and PBD/ID(H83L)	Rac1(T17N)
Growth rate	Mean ($\mu\text{m}/\text{min}$)	5.8 (± 2.7 , $n = 393$)	7.0 (± 3.6 , $n = 815$)	6.3 (± 3.2 , $n = 590$)	6.2 (± 2.7 , $n = 1043$)	5.2 (± 1.9 , $n = 457$)	6.3 (± 3.0 , $n = 396$)
	Median ($\mu\text{m}/\text{min}$)	5.1	6.0	5.2	5.5	4.6	5.5
Shortening rate	Mean ($\mu\text{m}/\text{min}$)	-12.1 (± 8.4 , $n = 179$)	-8.8 (± 7.5 , $n = 83$)	-10.2 (± 5.7 , $n = 284$)	-15.8 (± 12.7 , $n = 109$)	-7.6 (± 5.2 , $n = 145$)	-8.1 (± 3.8 , $n = 204$)
	Median ($\mu\text{m}/\text{min}$)	-10.1	-6.0	-9.3	-11.5	-6.0	-7.4
Catastrophe frequency (s^{-1})		0.052 ($n = 103$)	0.014 ($n = 59$)	0.047 ($n = 139$)	0.014 ($n = 73$)	0.044 ($n = 101$)	0.058 ($n = 115$)
Rescue frequency (s^{-1})		0.109 ($n = 98$)	0.145 ($n = 60$)	0.096 ($n = 136$)	0.129 ($n = 70$)	0.149 ($n = 108$)	0.110 ($n = 112$)
Time spent	Growing (%)	20.2	38.8	26.9	43.5	19.1	19.2
	Pausing (%)	70.6	57.2	60.1	52.0	74.9	71.0
	Shortening (%)	9.2	3.9	12.9	4.5	6.1	9.9
Net growth	Mean ($\mu\text{m}/\text{min}$)	0.0 (± 0.8)	2.4 (± 1.2)	0.2 (± 1.2)	2.0 (± 1.2)	0.5 (± 0.6)	0.4 (± 0.7)
Total time observed (min)		163	175	183	200	200	172
Number of cells, microtubules		4, 35	4, 35	4, 36	4, 40	4, 40	5, 35

n, total number of events observed. \pm indicates SD. In cells injected only with PBD/ID(H83L), dynamics parameters were determined from MTs in flat areas underneath neighboring cells. In all other conditions, MTs were analyzed in the free cell edge.

regulation of MT and actin dynamics in the leading edge of migrating cells.

Results and discussion

Rac1 activation promotes MT plus end growth and turnover in PtK1 cells

We used PtK1 cells, a marsupial kidney epithelial cell line, in which we observed EGF-stimulated Op18/stathmin phosphorylation (unpublished data), to study regulation of leading-edge MT dynamics. In control PtK1 cells injected with X-rhodamine-labeled tubulin and visualized by time-lapse fluorescence microscopy, we observed a subset of MTs that grew into leading-edge protrusions and behaved very similar to "pioneer" MTs in newt lung epithelial cells (Waterman-Storer and Salmon, 1997). The plus ends of these MTs experienced markedly less catastrophes and spent more time growing than the majority of MTs, which terminated further from the leading edge ("central" MTs; Fig. 1; Video 1, available at <http://www.jcb.org/cgi/content/full/jcb.200303082/DC1>; see also Fig. 4, E and F; Table I). In addition, in protruding cell areas, MTs exhibited retrograde flow relative to the cell edge.

To examine the role of Rac1 in the regulation of MT dynamics, we expressed a constitutively active Rac1 mutant, Rac1(Q61L). This induced the formation of a uniform lamellipodium all around the noncontacted edge of PtK1 cells, similar to what has been observed in fibroblasts (Hall, 1998). In Rac1(Q61L)-expressing cells, MTs were subjected to continuous, rapid, uniform retrograde flow toward the cell center, but most MT plus ends remained in close proximity to the cell edge (Fig. 2; Video 2). Although the plus ends of these MTs often appeared paused near the cell edge, the retrograde move-

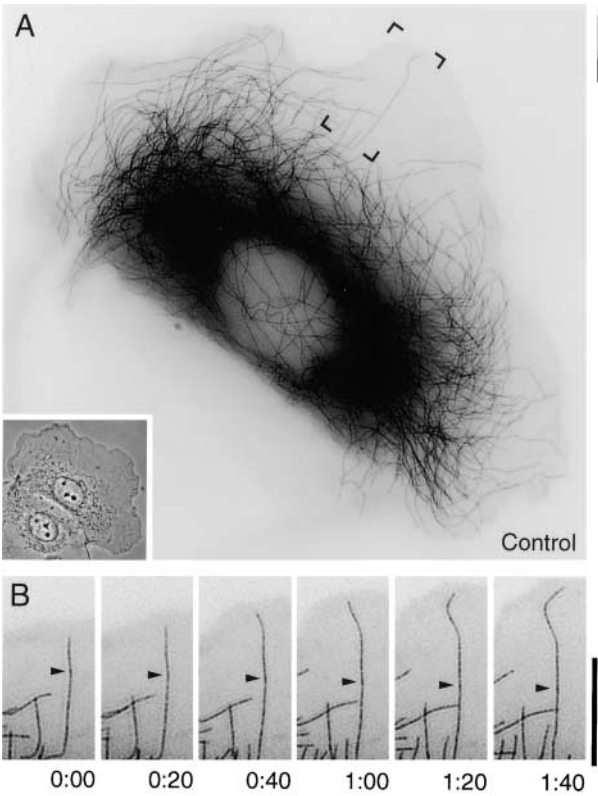


Figure 1. MT dynamics in a PtK1 cell. (A) MTs in a control PtK1 cell visualized by microinjected X-rhodamine tubulin and fluorescence microscopy (Video 1). Inset: phase contrast image of the same cell. (B) Dynamic behavior of MTs in the boxed area in A. A pioneer MT exhibits extensive plus end growth during protrusion of the leading edge. Arrow, fiduciary mark on the MT. Elapsed time, min:sec. Bars, 10 μm .

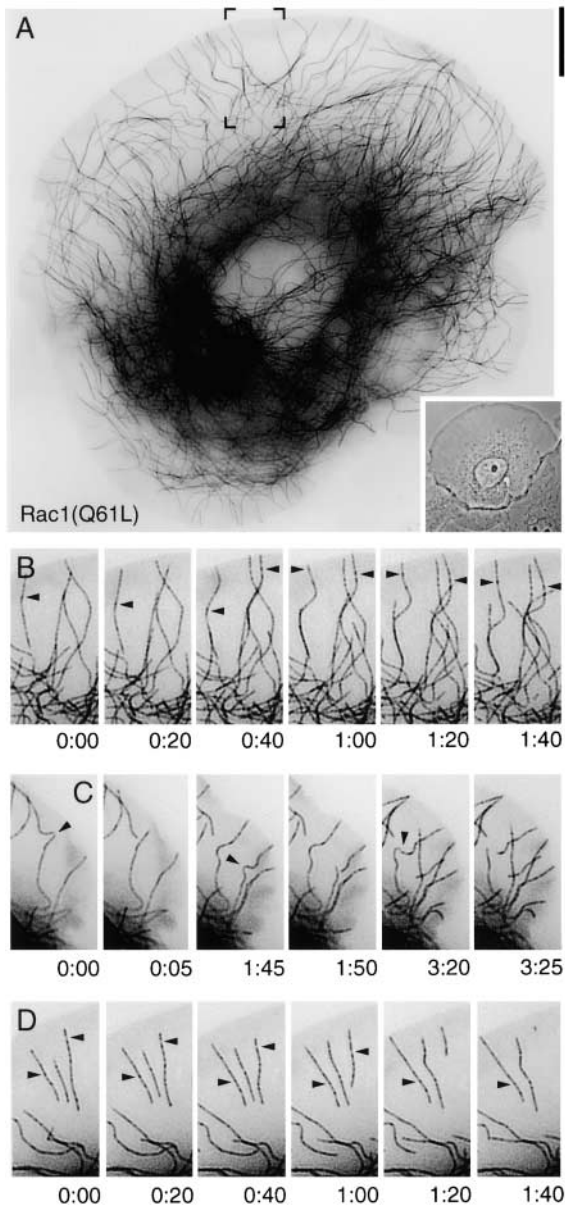


Figure 2. Constitutively active Rac1(Q61L) promotes MT growth at cell edges. (A) MTs in a PtK1 cell expressing constitutively active Rac1(Q61L) (Video 2). Inset: phase contrast image of the same cell. (B) Dynamic behavior of MTs in the boxed area in A. Although MT plus ends at the edge of Rac1(Q61L)-expressing cells often appear stationary, the constant rearward flow of fiduciary marks on the MT lattices (arrows) reveals that they are actively growing. (C) MTs buckle and break (arrows) as a result of retrograde flow in Rac1(Q61L)-expressing cells. (D) Treadmilling of MT fragments in a Rac1(Q61L)-expressing cell. Fragments eventually depolymerize by minus-end shortening (Video 5). Arrows indicate fiduciary marks on MTs. Elapsed time, min:sec. Bars, 10 μ m.

ment of fluorescent fiduciary marks on their lattices revealed that they were actually growing relatively steadily (Fig. 2, B and D). In contrast, cells expressing dominant-negative Rac1(T17N) had no lamellipodia, but a retracted morphology and exhibited no retrograde flow of MTs. In these cells, MT ends switched frequently between growth and shortening, with little net change in length over time (Fig. 3; Video 3). This difference in MT dynamic behavior was most evident

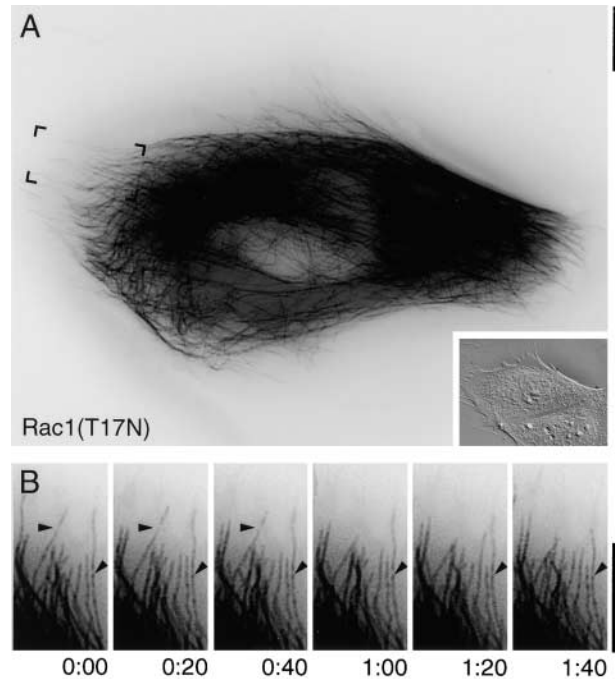


Figure 3. Dominant-negative Rac1(T17N) eliminates pioneer MT behavior. (A) MTs in a PtK1 cell expressing dominant-negative Rac1(T17N) (Video 3). Inset: differential interference contrast image of the same cell. (B) Dynamic behavior of MTs in the boxed area in A. MTs do not undergo retrograde flow and frequently transition between growth and shortening phases. Arrows, fiduciary marks on MTs. Elapsed time, min:sec. Bars, 10 μ m.

in a side-by-side comparison of cells expressing dominant-negative or constitutively active Rac1 (Video 4).

To quantitatively verify these observations, we measured dynamic instability parameters of individual MT plus ends, taking care to correct measurements for retrograde MT flow. This analysis revealed that nearly all MTs in constitutively active Rac1(Q61L)-expressing cells exhibited a kinetic behavior similar to pioneer MTs in control cells (Table I). This was characterized by a low catastrophe frequency and an increased percentage of time spent in growth, which resulted in high net plus-end growth (Fig. 4, E and F). In contrast, the dynamic behavior of most MTs in dominant-negative Rac1(T17N)-expressing cells was similar to central MTs in control cells, in which catastrophe frequency and the time spent in pause were high. These results indicate that Rac1 activation has major effects on MT dynamics, promoting net MT growth into leading lamellipodia by influencing specific parameters of MT dynamic instability. Localized Rac1 activation has been observed in the leading edge of migrating fibroblasts (Kraynov et al., 2000), and could also be present in epithelial cells, and therefore be responsible for the kinetic behavior of the subset of pioneer MTs in protruding cell edges.

Because this analysis clearly demonstrated that Rac1 activation promoted net MT polymerization in the cell periphery, we reasoned that increased MT depolymerization must occur elsewhere in cells expressing constitutively active Rac1(Q61L) to maintain a stable polymer level. Indeed, careful observation of MTs in Rac1(Q61L)-expressing cells

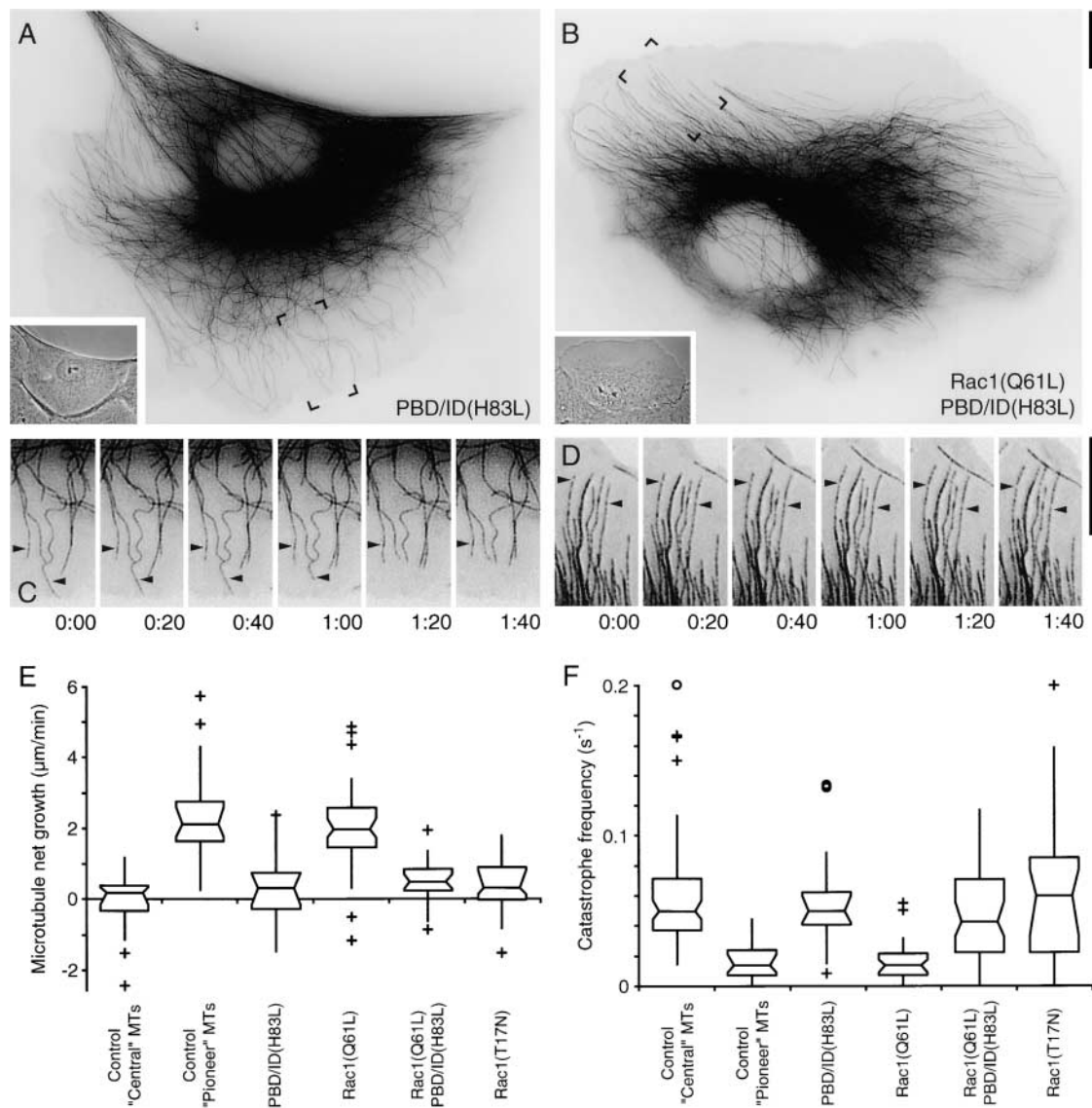


Figure 4. Pak inhibition blocks Rac1(Q61L)-mediated MT growth. (A) MTs in a PtK1 cell injected with the Pak1 inhibitory fragment PBD/ID(H83L) (120 μ M needle concentration) and X-rhodamine tubulin (Video 6). Note that the boxed area represents a flat region underneath a neighboring cell. (B) MTs in a Rac1(Q61L)-expressing PBD/ID(H83L)-injected PtK1 cell (Video 7). Insets: phase contrast images of the cells in A and B. (C) Dynamic behavior of MTs in the boxed area in A. MTs grow very little and do not exhibit retrograde flow in PBD/ID(H83L)-injected cells. (D) Dynamic behavior of MTs in the boxed area in B. In Rac1(Q61L)-expressing PBD/ID(H83L)-injected cells, retrograde MT flow is severely reduced and MTs grow very little. Arrows, fiduciary marks on MTs. Elapsed time, min:sec. Bars, 10 μ m. (E, F) Statistical evaluation of MT net growth (E) and catastrophe frequency (F) of individual MTs (from Table I). Net MT growth is significantly reduced and the catastrophe frequency increased in cells expressing Rac1(T17N) or injected with the Pak1 inhibitory fragment as compared with pioneer MTs or MTs in Rac1(Q61L)-expressing cells ($P < 0.01$ by ANOVA). Data in this and the next figure are presented as box-and-whisker plots indicating the 25th percentile (bottom boundary), median (middle line), 75th percentile (top boundary), nearest observations within 1.5 times the interquartile range (whiskers), 95% confidence interval of the median (notches), and near (+) and far (○) outliers.

revealed that MT buckling and breakage occurred frequently in the proximal lamellum as a result of compressive forces exerted on MTs by increased retrograde flow (Fig. 2 C; Gupton et al., 2002). MT breakage created free MT minus ends that either paused or shortened, but never grew (Waterman-Storer and Salmon, 1997), resulting in net "treadmilling" of many dynamically unstable MT fragments (Fig. 2 D; Video 5). The net rate of minus-end shortening was slightly higher than that of net plus-end growth (2.4 μ m/min versus 2.0 μ m/min), suggesting that such fragments eventually depolymerize completely. The notion of in-

creased MT turnover in Rac1(Q61L)-expressing cells was also supported by the observation that the total amount of MT polymer was slightly but significantly ($P < 0.001$ by ANOVA) reduced in cells expressing constitutively active Rac1(Q61L) ($58 \pm 5\%$, $n = 93$ cells) as compared with control cells ($65 \pm 5\%$, $n = 104$) or cells expressing dominant-negative Rac1(T17N) ($63 \pm 7\%$, $n = 24$).

Similar to our current finding that Rac1-dependent increases in MT retrograde flow promote MT turnover, pharmacological treatment of newt lung cells that resulted in an increased rate of retrograde flow also increased MT breakage

and turnover (Gupton et al., 2002). This supports the idea that retrograde flow-induced MT breakage may be a major pathway for MT turnover in migrating cells.

Pak inhibition blocks Rac1(Q61L)-induced MT growth

To determine if Paks mediated these dramatic Rac1 effects on MT plus-end growth and retrograde flow, we analyzed individual MT dynamics in control and Rac1(Q61L)-expressing cells injected with a mutated fragment of Pak1,

PBD/ID(H83L), that inhibits the kinase activity of Paks, but cannot sequester activated Rac1 (Zenke et al., 1999). In PtK1 cells, Pak inhibition often caused complete retraction of the lamellum (Fig. 4, A and C; Video 6), but did not have this effect in cells expressing constitutively active Rac1(Q61L) (Fig. 4, B and D; Video 7). However, either Pak inhibition alone or in combination with Rac1(Q61L) expression resulted in MTs spending less time growing and exhibiting an increased catastrophe frequency, resulting in

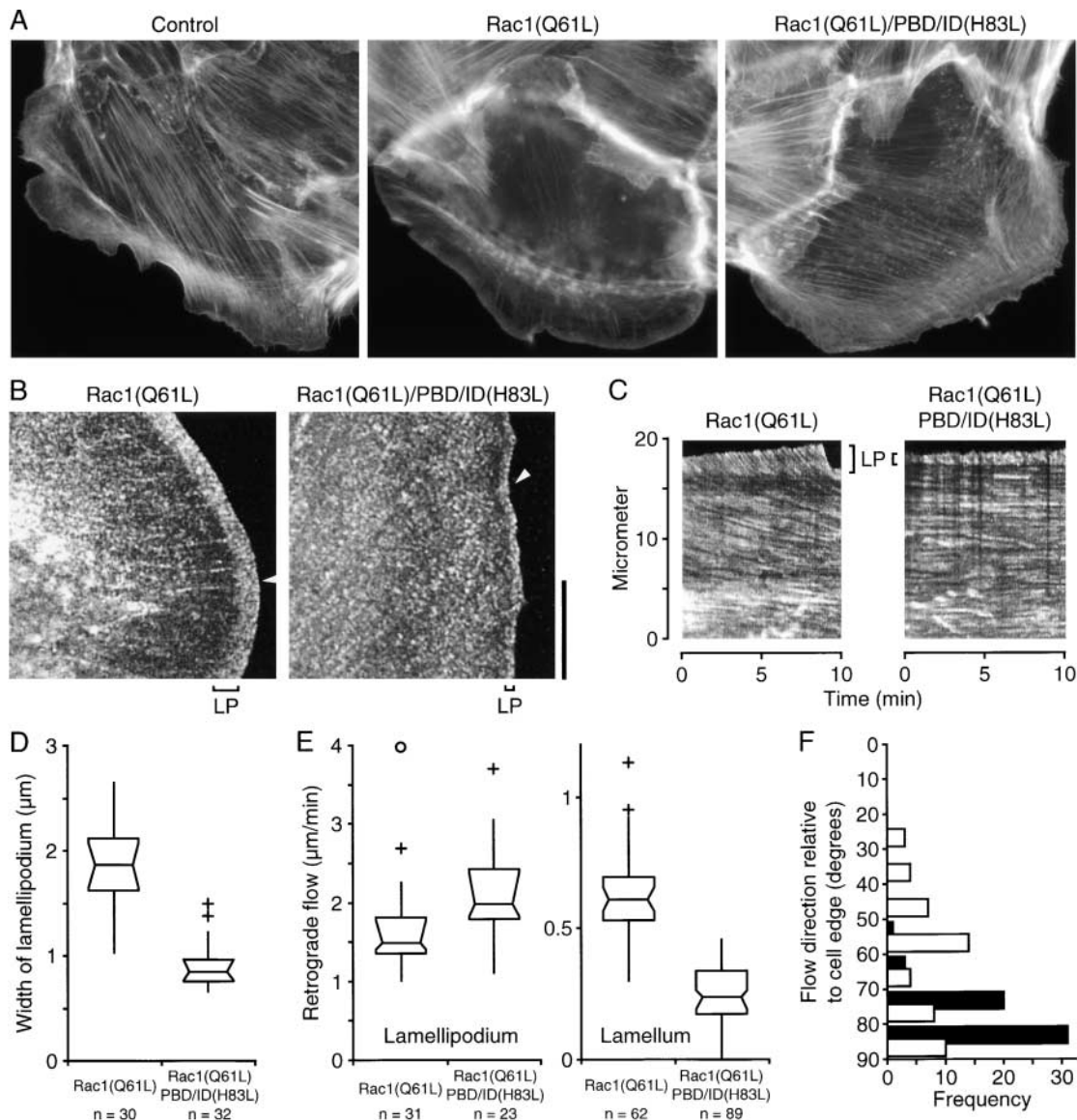


Figure 5. Pak inhibition blocks Rac1(Q61L)-induced actin dynamics. (A) Control, Rac1(Q61L)-, and Rac1(Q61L)-expressing PtK1 cells injected with PBD/ID(H83L) were fixed and stained with fluorescent phalloidin. Pak inhibition blocks Rac1(Q61L)-induced concentration of actin in the lamellipodium and promotes the formation of parallel actin bundles in the cell body. (B) Single frames of actin fluorescent speckle time-lapse series of Rac1(Q61L)-expressing cells injected with GST or PBD/ID(H83L) (Videos 8 and 9). LP, lamellipodium. Bars, 10 μm . (C) Kymograph analysis of actin retrograde flow in the cells in B along the lines indicated by arrowheads. Streaks on kymographs indicate speckle position over time; steeper streaks = faster flow rate. (D) Width of the lamellipodium in Rac1(Q61L)-expressing cells and PBD/ID(H83L)-injected, Rac1(Q61L)-expressing cells measured in fixed, phalloidin-stained cells. Inhibition of Pak downstream of Rac1 reduces the lamellipodium width. *n*, number of cells analyzed. (E) Rate of actin retrograde flow in the lamellipodium and lamellum in Rac1(Q61L)-expressing cells and PBD/ID(H83L)-injected, Rac1(Q61L)-expressing cells. Inhibition of Pak reduces the rate of flow in the lamellum but not the lamellipodium. *n*, number of measurements from kymographs in 10 cells. (F) Histogram of the direction of lamella actin flow relative to the cell edge in Rac1(Q61L)-expressing cells (solid bars) and PBD/ID(H83L)-injected, Rac1(Q61L)-expressing cells (open bars). Actin retrograde flow is predominantly perpendicular to the edge in Rac1(Q61L)-expressing cells but residual flow is randomized on Pak inhibition.

decreased MT net growth as compared with MTs in Rac1(Q61L)-expressing cells or pioneer MTs in control cells (Fig. 4, E and F; Table I). In addition, Pak inhibition blocked Rac1(Q61L)-accelerated MT retrograde flow, buckling, and breakage, which returned the total MT polymer level ($68 \pm 6\%$, $n = 35$) to what we observed in control cells, indicating that Pak is required for Rac1(Q61L)-mediated increase in MT turnover. As a control, we found that an inactivated Pak inhibitor, PBD/ID(H83L, L107F), did not affect MT dynamics in Rac1(Q61L)-expressing cells. Thus, Pak activation is required for the promotion of pioneer MT dynamics downstream of Rac1.

To determine if Paks were the sole regulators of MT dynamics downstream of Rac1, we examined the effects of various constitutively active forms of Pak1, Pak1(T423E), or Pak1(H83L, H86L) (Sells et al., 1999) and their membrane-targeted CAAX-box fusions, on the dynamics of individual MTs in PtK1 cells. However, we could not observe a consistent effect on MT organization or dynamic behavior as compared with control cells (unpublished data), indicating that although Pak activation is necessary for Rac1-induced MT plus-end growth, constitutively active Pak1 alone is not sufficient. This suggests that Pak-mediated phosphorylation and inactivation of Op18/stathmin might not be the major regulatory mechanism for leading edge MT dynamics induced by Rac1 (Daub et al., 2001). However, expression of constitutively active Pak1 likely caused high Pak1 activity globally throughout the cell, but local regulation of cytoskeletal dynamics at the leading edge may require local activation of Paks (Sells et al., 2000). Thus, constitutively active Pak1 could have simply caused a shift to a new global equilibrium in which MT plus-end dynamics might be similar to control cells. In addition, constitutively active Pak1 did not promote obvious changes of cell morphology or lamellipodial protrusion as it has been observed in fibroblasts (Sells et al., 1999). This indicates that multiple pathways regulating cytoskeletal dynamics downstream of Rac1 must exist, and is consistent with the apparently complicated role of Paks in the regulation of actin contraction and polymerization dynamics (Bokoch, 2003).

Paks regulate actin retrograde flow downstream of Rac1

Because altering the activity of Rac1 and downstream inhibition of Paks affected MT retrograde flow, we hypothesized that this was due to coupling of MT movements to those of the actin cytoskeleton (Gupton et al., 2002; Salmon et al., 2002). Therefore, we examined actin organization and dynamics in cells expressing constitutively active Rac1(Q61L), as compared with such cells additionally injected with the Pak inhibitor PBD/ID(H83L). First, we fixed and stained cells with fluorescent phalloidin. Rac1(Q61L) expression induced the formation of a dense F-actin meshwork in the lamellipodium and of transverse bundles at the base of the lamellum (Fig. 5 A). When PBD/ID(H83L) was injected into Rac1(Q61L)-expressing cells, the transverse actin bundles were lost in 90% of the cells and the width of the lamellipodium was reduced significantly ($1.9 \pm 0.4 \mu\text{m}$ versus $0.9 \pm 0.2 \mu\text{m}$; Fig. 5 D). In addition, extensive parallel actin bundles that stretched from the cell body to the lamellipodium formed in >60% of injected cells (Fig. 5 A) (Zhao

et al., 1998). The F-actin organization in control PtK1 cells appeared to be a hybrid of these two phenotypes.

Then, we directly observed actin dynamics by confocal fluorescent speckle microscopy in cells injected with low levels of X-rhodamine-labeled actin (Waterman-Storer et al., 1998). In Rac1(Q61L)-expressing cells, actin underwent fast flow in the lamellipodium ($1.67 \pm 0.57 \mu\text{m}/\text{min}$) and slow retrograde flow in the lamellum ($0.63 \pm 0.16 \mu\text{m}/\text{min}$; Fig. 5, B and C; Video 8; Salmon et al., 2002). Although Pak inhibition did not reduce the rate of actin retrograde flow in the thin remaining lamellipodium ($2.14 \pm 0.61 \mu\text{m}/\text{min}$), indicating that it has no effect on actin polymerization, flow in the lamellum, which is likely to be myosin dependent (Waterman-Storer and Salmon, 1997), decreased almost threefold ($0.25 \pm 0.12 \mu\text{m}/\text{min}$; Fig. 5, B, C, and E; Video 9). This is consistent with a role of Paks in myosin phosphorylation (Bokoch, 2003). Furthermore, the remaining flow was not predominantly perpendicular to the leading edge as we observed in Rac1(Q61L)-expressing cells (Fig. 5 F). The reduction of lamellipodial width also suggests that Pak inhibition may increase filament depolymerization and the rate of treadmilling through inhibition of Lim kinase, and thus activation of cofilin (Bokoch, 2003).

Together, these results indicate that Pak activity is required for Rac1-induced changes in actin and MT organization and dynamics. In this paper, we have shown that Rac1 activation promotes Pak-dependent MT growth in epithelial cells. However, the underlying molecular mechanism remains to be defined, and is likely to involve more than one MT regulatory protein. In addition, dynamic interactions between MTs and the actin cytoskeleton might be required for pioneer MT behavior to occur. Our previous work has shown that MT growth can activate Rac1 in tissue cells by a yet unknown mechanism (Waterman-Storer et al., 1999). Thus, a decrease in Rac1 activity could be responsible for the inhibition of protrusion in the absence of MTs. Together with our current results, this suggests that Rac1 and MT growth might constitute a positive feedback loop in which MT growth promotes Rac1 activation and Rac1 promotes further MT growth to reinforce the polarization of a migrating cell in the absence of extracellular signals.

Materials and methods

Cell culture and microinjection

PtK1 cells were cultured in Ham's F12 medium containing 25 mM Hepes (Sigma-Aldrich) and 10% FBS (GIBCO BRL) at 37°C, 5% CO₂. pcDNA3 mammalian expression vectors (Invitrogen) encoding EGFP-Rac1(Q61L) or EGFP-Rac1(T17N) (from Klaus Hahn, The Scripps Research Institute) were injected into the cell nucleus at 100 $\mu\text{g}/\text{ml}$. X-rhodamine-conjugated tubulin and actin were prepared as described previously (Waterman-Storer, 2002) and injected at 1 mg/ml . In some experiments, plasmid and fluorescent protein were coinjected into the nucleus. GST-PBD/ID(H83L) (aa 67–150 of human Pak1) was expressed and purified as described previously (Zenke et al., 1999), dialyzed against 50 mM potassium glutamate, pH 7.0, 0.5 mM MgCl₂, 100 mM KCl, and 0.5 mM DTT, and concentrated on Aquacide II (Calbiochem). Injection with GST-PBD/ID(H83L) was confirmed by anti-GST immunostaining after the experiment. The MT polymer-to-dimer ratio was determined as described previously (Zhai and Borisy, 1994).

Microscopy and image analysis

Cells were maintained on the microscope stage in aluminum slide chambers in culture medium containing 0.5–1.0 U oxyrase per ml (Oxyrase, Inc.)

to inhibit photobleaching and kept at 35–37°C with an air stream incubator (Nevtek). To measure MT dynamic instability parameters, epifluorescence image series were acquired on an inverted microscope (model TE300; Nikon) equipped with electronically controlled shutters, filter wheels, and a 14-bit cooled CCD camera (Orca II; Hamamatsu Corporation) controlled by MetaMorph® software (Universal Imaging Corp.) at 5-s intervals using a 60×/1.4 NA Plan Apo objective lens (Nikon). Actin fluorescent speckle time-lapse series were acquired on a spinning disk confocal microscope (Adams et al., 2003) with a 100×/1.4 NA Plan Apo objective lens, and images were processed as described previously (Salmon et al., 2002).

Images in MT time-lapse sequences were registered relative to fiducial marks on the MT lattices such that tracking of the MT ends accurately measured plus end dynamics without the bias of retrograde MT flow. Approximately 10 MTs that remained visible for several minutes were tracked in each cell using the MetaMorph® “track points” function, and data were analyzed in Excel (Microsoft) with a custom-written macro. Only MT length changes exceeding the optical resolution limit of 0.25 μm per frame (3 μm/min) were considered growth or shortening events, and rates were calculated as instantaneous velocities for each pair of consecutive image frames. Transition events from pause to shortening (or growth) were only classified as catastrophes (or rescues) if growth (or shortening) preceded the pause. The catastrophe (or rescue) frequency was defined as number of catastrophes (or rescues) divided by the time the MT spent growing (or shortening). Images for presentation and movie sequences were contrast inverted and subjected to an “unsharp mask” filter.

Online supplemental material

Video 1 shows MTs in a control PtK1 cell (Fig. 1). Video 2 shows MTs in a constitutively active Rac1(Q61L)-expressing PtK1 cell (Fig. 2). Video 3 shows MTs in a dominant-negative Rac1(T17N)-expressing PtK1 cell (Fig. 3). Video 4 shows direct comparison of MT dynamics in PtK1 cells expressing Rac1(Q61L) or Rac1(T17N). Video 5 shows MT fragments exhibiting net treadmilling in a Rac1(Q61L)-expressing PtK1 cell (Fig. 2 D). Video 6 shows MTs in a PtK1 cell injected with the Pak inhibitory fragment PBD/ID(H83L) (Fig. 4, A and C). Video 7 shows MTs in a PBD/ID(H83L)-injected, Rac1(Q61L)-expressing PtK1 cell (Fig. 4, B and D). Video 8 shows actin dynamics in a Rac1(Q61L)-expressing PtK1 cell (Fig. 5 B). Video 9 shows actin dynamics in a PBD/ID(H83L)-injected, Rac1(Q61L)-expressing PtK1 cell (Fig. 5 B). Online supplemental material available at <http://www.jcb.org/cgi/content/full/jcb.200303082/DC1>.

We thank Søren Andersen, Arshad Desai, Martin Gullberg, Mira Krendel, and members of the Waterman-Storer lab for discussions and comments on the manuscript.

This work was funded by National Institutes of Health grants GM61804 to C.M. Waterman-Storer, GM39434 to G.M. Bokoch, and an EMBO Long Term fellowship to T. Wittmann.

Submitted: 12 March 2003

Revised: 24 April 2003

Accepted: 28 April 2003

References

Adams, M.C., W.C. Salmon, S.L. Gupton, C.S. Cohan, T. Wittmann, N. Prigozhina, and C.M. Waterman-Storer. 2003. A high-speed multispectral spinning-disk confocal microscope system for fluorescent speckle microscopy of living cells. *Methods*. 29:29–41.

Ballemstrem, C., B. Wehrle-Haller, B. Hinz, and B.A. Imhof. 2000. Actin-dependent lamellipodia formation and microtubule-dependent tail retraction control directed cell migration. *Mol. Biol. Cell*. 11:2999–3012.

Bokoch, G.M. 2003. Biology of the p21-activated kinases. *Annu. Rev. Biochem.* 72: 743–781.

Daub, H., K. Gevaert, J. Vandekerckhove, A. Sobel, and A. Hall. 2001. Rac/Cdc42 and p65PAK regulate the microtubule-destabilizing protein stathmin through phosphorylation at serine 16. *J. Biol. Chem.* 276:1677–1680.

Desai, A., and T.J. Mitchison. 1997. Microtubule polymerization dynamics. *Annu. Rev. Cell Dev. Biol.* 13:83–117.

Etienne-Manneville, S., and A. Hall. 2001. Integrin-mediated activation of Cdc42 controls cell polarity in migrating astrocytes through PKC ζ . *Cell*. 106:489–498.

Gupton, S.L., W.C. Salmon, and C.M. Waterman-Storer. 2002. Converging populations of F-actin promote breakage of associated microtubules to spatially regulate microtubule turnover in migrating cells. *Curr. Biol.* 12:1891–1899.

Hall, A. 1998. Rho GTPases and the actin cytoskeleton. *Science*. 279:509–514.

Kraynov, V.S., C. Chamberlain, G.M. Bokoch, M.A. Schwartz, S. Slabaugh, and K.M. Hahn. 2000. Localized Rac activation dynamics visualized in living cells. *Science*. 290:333–337.

Palazzo, A.F., H.L. Joseph, Y.J. Chen, D.L. Dujardin, A.S. Alberts, K.K. Pfister, R.B. Vallee, and G.G. Gundersen. 2001a. Cdc42, dynein, and dynactin regulate MTOC reorientation independent of Rho-regulated microtubule stabilization. *Curr. Biol.* 11:1536–1541.

Palazzo, A.F., T.A. Cook, A.S. Alberts, and G.G. Gundersen. 2001b. mDia mediates Rho-regulated formation and orientation of stable microtubules. *Nat. Cell Biol.* 3:723–729.

Ridley, A.J. 2001. Rho GTPases and cell migration. *J. Cell Sci.* 114:2713–2722.

Salmon, W.C., M.C. Adams, and C.M. Waterman-Storer. 2002. Dual-wavelength fluorescent speckle microscopy reveals coupling of microtubule and actin movements in migrating cells. *J. Cell Biol.* 158:31–37.

Sells, M.A., J.T. Boyd, and J. Chernoff. 1999. p21-activated kinase 1 (Pak1) regulates cell motility in mammalian fibroblasts. *J. Cell Biol.* 145:837–849.

Sells, M.A., A. Pfaff, and J. Chernoff. 2000. Temporal and spatial distribution of activated Pak1 in fibroblasts. *J. Cell Biol.* 151:1449–1458.

Small, J.V., T. Stradal, E. Vignal, and K. Rottner. 2002. The lamellipodium: where motility begins. *Trends Cell Biol.* 12:112–120.

Wadsworth, P. 1999. Regional regulation of microtubule dynamics in polarized, motile cells. *Cell Motil. Cytoskeleton*. 42:48–59.

Waterman-Storer, C.M. 2002. Fluorescent speckle microscopy (FSM) of microtubules and actin in living cells. In *Current Protocols in Cell Biology*. K.S. Morgan, editor. John Wiley & Sons Inc., New York. 4.10.1–4.10.26.

Waterman-Storer, C.M., and E.D. Salmon. 1997. Actomyosin-based retrograde flow of microtubules in the lamella of migrating epithelial cells influences microtubule dynamic instability and turnover and is associated with microtubule breakage and treadmilling. *J. Cell Biol.* 139:417–434.

Waterman-Storer, C.M., A. Desai, J.C. Bulinski, and E.D. Salmon. 1998. Fluorescent speckle microscopy, a method to visualize the dynamics of protein assemblies in living cells. *Curr. Biol.* 8:1227–1230.

Waterman-Storer, C.M., R.A. WorthyLake, B.P. Liu, K. Burridge, and E.D. Salmon. 1999. Microtubule growth activates Rac1 to promote lamellipodial protrusion in fibroblasts. *Nat. Cell Biol.* 1:45–50.

Wittmann, T., and C.M. Waterman-Storer. 2001. Cell motility: can Rho GTPases and microtubules point the way? *J. Cell Sci.* 114:3795–3803.

Zenke, F.T., C.C. King, B.P. Bohl, and G.M. Bokoch. 1999. Identification of a central phosphorylation site in p21-activated kinase regulating autoinhibition and kinase activity. *J. Biol. Chem.* 274:32565–32573.

Zhai, Y., and G.G. Borisy. 1994. Quantitative determination of the proportion of microtubule polymer present during the mitosis-interphase transition. *J. Cell Sci.* 107:881–890.

Zhao, Z.S., E. Manser, X.Q. Chen, C. Chong, T. Leung, and L. Lim. 1998. A conserved negative regulatory region in α PAK: inhibition of PAK kinases reveals their morphological roles downstream of Cdc42 and Rac1. *Mol. Cell. Biol.* 18:2153–2163.